

# Ecology-guided prediction of cross-feeding interactions in the human gut microbiome

**Akshit Goyal**

Physics of Living Systems, Massachusetts Institute of Technology, Cambridge, MA 02139, USA

**Tong Wang**

Department of Bioengineering and Carl R. Woese Institute for Genomic Biology, University of Illinois at Urbana-Champaign, Urbana, IL 61801, USA

**Veronika Dubinkina**

Department of Bioengineering and Carl R. Woese Institute for Genomic Biology, University of Illinois at Urbana-Champaign, Urbana, IL 61801, USA

**Sergei Maslov** (✉ [maslov@illinois.edu](mailto:maslov@illinois.edu))

Department of Bioengineering and Carl R. Woese Institute for Genomic Biology, University of Illinois at Urbana-Champaign, Urbana, IL 61801, USA <https://orcid.org/0000-0002-3701-492X>

---

## Article

**Keywords:** human gut microbiome, metabolites, GutCP, ecology-based computational method

**Posted Date:** July 1st, 2020

**DOI:** <https://doi.org/10.21203/rs.3.rs-38434/v1>

**License:** © ⓘ This work is licensed under a Creative Commons Attribution 4.0 International License.

[Read Full License](#)

---

**Version of Record:** A version of this preprint was published at Nature Communications on February 26th, 2021. See the published version at <https://doi.org/10.1038/s41467-021-21586-6>.

# Ecology-guided prediction of cross-feeding interactions in the human gut microbiome

Akshit Goyal<sup>1,†</sup>, Tong Wang<sup>2,†</sup>, Veronika Dubinkina<sup>2</sup>, and Sergei Maslov<sup>2,\*</sup>

<sup>1</sup>*Physics of Living Systems, Massachusetts Institute of Technology, Cambridge, MA 02139, USA.*

<sup>2</sup>*Department of Bioengineering and Carl R. Woese Institute for Genomic Biology, University of Illinois at Urbana-Champaign, Urbana, IL 61801, USA.*

† These authors contributed equally.

\* Correspondence to: [maslov@illinois.edu](mailto:maslov@illinois.edu).

(Dated: June 8, 2020)

Understanding a complex microbial ecosystem such as the human gut microbiome requires information about both microbial species and the metabolites they produce and secrete. These metabolites are exchanged via a large network of cross-feeding interactions, and are crucial for predicting the functional state of the microbiome. However, till date, we only have information for a part of this network, limited by experimental throughput. Here, we propose an ecology-based computational method, GutCP, using which we predict hundreds of new experimentally untested cross-feeding interactions in the human gut microbiome. GutCP utilizes a mechanistic model of the gut microbiome with the explicit exchange of metabolites and their effects on the growth of microbial species. To build GutCP, we combined metagenomic and metabolomic measurements from the gut microbiome with optimization techniques from machine learning. Close to 65% of the cross-feeding interactions predicted by GutCP are supported by evidence from genome annotation; we provide these predictions for experimentally testing. Our method has the potential to greatly improve existing models of the human gut microbiome, as well as our ability to predict the metabolic profile of the gut.

The gut microbiome plays an important role in human health, and the ability to manipulate it holds immense potential to prevent and treat multiple diseases<sup>1–8</sup>. The microbiome comprises not only of hundreds of microbial species, but also hundreds of metabolites that they consume and secrete: a phenomenon called cross-feeding<sup>9,10</sup>. These metabolites — through which gut microbes interact with each other — mediate inter-species interactions and can even directly impact the host<sup>11–14</sup>. Indeed, metabolite levels in the gut are often more predictive of host health than species levels<sup>11,15,16</sup>. Therefore, developing a complete understanding of both the human gut microbiome together with the metabolome is necessary to positively control and manipulate human health.

A promising framework to realize such an understanding is a fully mechanistic model of the microbiome<sup>17–20</sup>, which can connect the levels of microbial species and metabolites with each other quantitatively. An essential first step in building this model is establishing which metabolic interactions are relevant in the human gut microbiome<sup>18,20–22</sup>. Indeed, inferring cross-feeding interactions is an active and important field of microbiome research, and employs both direct<sup>9,23–25</sup> and indirect<sup>11,26–29</sup> inference methods. Direct methods, which comprise experimental verification of the metabolic activity of gut microbes, are slow, require painstaking effort, and thus miss many relevant interactions (i.e., they are incomplete). Indirect methods, which chiefly comprise inferring the metabolic activity of gut microbes from their genome sequences, are noisy, lack curation and vastly overestimate relevant cross-feeding interactions (i.e., they are “beyond complete”)<sup>30–32</sup>. We thus need new methods that represent the middle ground

between direct and indirect methods. Specifically, we need methods that can use the directly-inferred but incomplete interactions as a “bootstrap”, allowing one to filter out the indirectly-inferred but noisy ones. We believe that ecological consumer-resource models provide the means to perform this bootstrapping and predict new and ecologically sound cross-feeding interactions. Moreover, we believe that these methods can benefit from advances in machine learning<sup>33,34</sup>, which is effective at identifying patterns in known data and using them to make new predictions.

Here, we propose GutCP, short for Gut Cross-feeding Predictor: a new, general, and ecology-guided method to infer and predict cross-feeding interactions in the human gut microbiome. GutCP combines machine learning techniques<sup>33,34</sup> with an ecological model of the microbiome. The ecological model is effective at bootstrapping previously-known direct interactions and estimating the metabolic environment of the gut in agreement with experimental measurements<sup>20</sup>. GutCP uses these estimates as a leverage to predict new cross-feeding interactions. The machine learning techniques that GutCP employs help optimize and curate the process of inferring new interactions. We find that close to 65% of the interactions we predict are supported by the available genomic evidence. Our predictions can be easily tested by simple experiments, and have the potential to enable a fully mechanistic understanding of the human gut microbiome going beyond the analysis of correlations between species and metabolites.

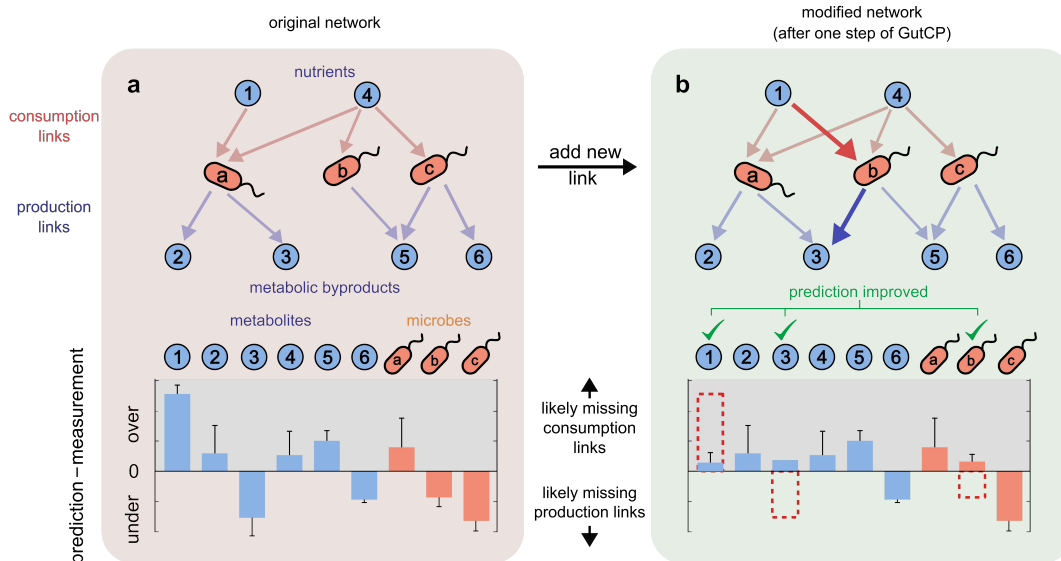


FIG. 1. **Overview of the GutCP algorithm.** **a**, Schematic of the original set of known cross-feeding interactions (top) and bar plot of the prediction error for each metabolite and microbe (bottom). The cross-feeding interactions are represented as a network, whose nodes are either metabolites (cyan circles) or microbial species (orange ellipses), and directed links represent abilities of different species to consume (red arrows) and produce (blue arrows) individual metabolites. **b**, GutCP adds a new consumption link (red) and production link (blue) as added links reduce the prediction errors for metabolites and microbes.

## RESULTS

**Overview of the GutCP algorithm.** Our approach uses the idea that we can leverage cross-feeding interactions — which comprise knowing the metabolites that each microbial species is capable of consuming and producing — to mechanistically connect the levels of microbes and metabolites in the human gut. Several different mechanistic models in past studies have shown that this is indeed possible<sup>18,20,29,35,36</sup>. While GutCP is generalizable and can be used with any of these models, in this manuscript, we use a previously published consumer-resource model<sup>20</sup>. We use this model because of its context and performance: it is built specifically for the human gut, and is best able to connect the experimentally measured species composition of the gut microbiome with its resulting metabolic environment, or fecal metabolome. To predict the metabolome from the microbiome, it relies on a manually-curated set of known cross-feeding interactions<sup>9</sup>. It then uses these known interactions to follow the step-wise flow of metabolites through the gut. At each step (ecologically, at each trophic level), the metabolites available to the gut are utilized by microbial species that are capable of consuming them, and a fraction of these metabolites are secreted as metabolic byproducts. These byproducts are then available for consumption by another set of species in the next trophic level. After several such steps, the metabolites that are left unconsumed constitute the fecal metabolome.

We hypothesized that adding new, yet-undiscovered cross-feeding interactions would improve our ability to

connect the levels of microbes and metabolites with our mechanistic and causal model. Specifically, we predict that the set of undiscovered links resulting in the most accurate and optimal connection would be the most likely candidates for new cross-feeding interactions. Inferring such an optimal set of new cross-feeding interactions is the main logic driving GutCP. In what follows, we sometimes refer to cross-feeding interactions as “links” in an overall cross-feeding network of the gut microbiome, whose nodes are microbes and metabolites (Fig. 1a; metabolites in blue, microbes in orange); the links themselves are directed edges connecting the nodes. Links can be of two types: consumption links (from nutrients to microbes) and production links (from microbes to their metabolic byproducts).

The salient aspects of our method are outlined in Fig. 1. Briefly, we start with the known set of cross-feeding interactions which were originally used by the model; these links are known from direct experiments, and represent a ground truth dataset<sup>9</sup>. These are shown in Fig. 1a through the pink and blue arrows connecting nutrients 1 through 6 with microbes a through c. For each sample, using only the species abundance from the microbiome, we use the model to quantitatively estimate the microbiome’s species and metabolomic composition. For each metabolite and microbial species, there can be two kinds of prediction errors, or biases: individual (sample-specific difference between predicted and measured levels) and systematic (average difference across all samples). We focused on the “systematic bias” for each metabolite and microbial species: the average de-

viation of the predicted levels from the measured levels across all samples in our dataset (Fig. 1a, bottom). The systematic bias for each metabolite and microbe tells us whether our model generally tends to predicts their level to be greater than observed (over-predicted), less than observed (under-predicted), or neither (well-predicted). We assume that metabolites and microbes with a large systematic bias are most likely to harbor missing interactions. We prioritize adding links to them in proportion to their systematic biases.

After measuring the systematic bias for each metabolite and microbe, GutCP proceeds in discrete steps (Fig. 1a–b). At each step, we attempt to add a new link to the current cross-feeding network. We accept this link — keeping it in the current network — if it leads to an overall improvement in the agreement between the predicted and measured levels of microbes and metabolites. We repeat the process of adding new links — accepting or rejecting them — until the improvements in the levels of metabolites and microbes became insignificant. Overall, GutCP can add several links to improve the agreement between the predicted and measured levels of microbes and metabolites (in Fig. 1a–b, bottom, adding the extra red and blue link at the top results in improved predictions for metabolite 1, metabolite 3, and microbe *b*). Fig. 2a shows how the cross-feeding network improves over a typical GutCP run via the red trajectory, starting from the original network (Fig. 2a, top left) to the a final network state (Fig. 2a, bottom right). Trajectories from 100 other runs are shown in grey. GutCP repeatedly reduces both the error of the metabolome predictions ( $y$ -axis; measured as  $\log_{10}(\frac{\text{pred}-\text{meas}}{\text{measurement}})$ ) and improves the correlation between the predicted and measured metabolomes ( $x$ -axis).

### Cross-validating the newly predicted interactions.

To test if the cross-feeding interactions predicted by GutCP are generalizable to unknown datasets, we performed 4-fold cross-validation. As a proof-of-concept,

	metabolome pred – exp	log error	# of pred metabolites
original set	0.61	0.89	17
training set	$0.72 \pm 0.03$	$0.54 \pm 0.02$	$30 \pm 3$
test set	$0.68 \pm 0.04$	$0.59 \pm 0.04$	$30 \pm 3$

TABLE I. **Cross-validating the newly predicted interactions.** Table showing the performance of the ecological cross-feeding model with the original set of interactions, and with the additional interactions predicted by GutCP (both the training and test set performances; see main text). Performance is measured using three metrics: (1) the correlation between the predicted and experimentally measured metabolome, (2) the log error (see main text), and (3) the number of metabolites in the measured metabolome predicted by our ecological consumer-resource model. Values indicate mean for (1) and (2), and median for (3); errors, where shown, indicate standard deviation.

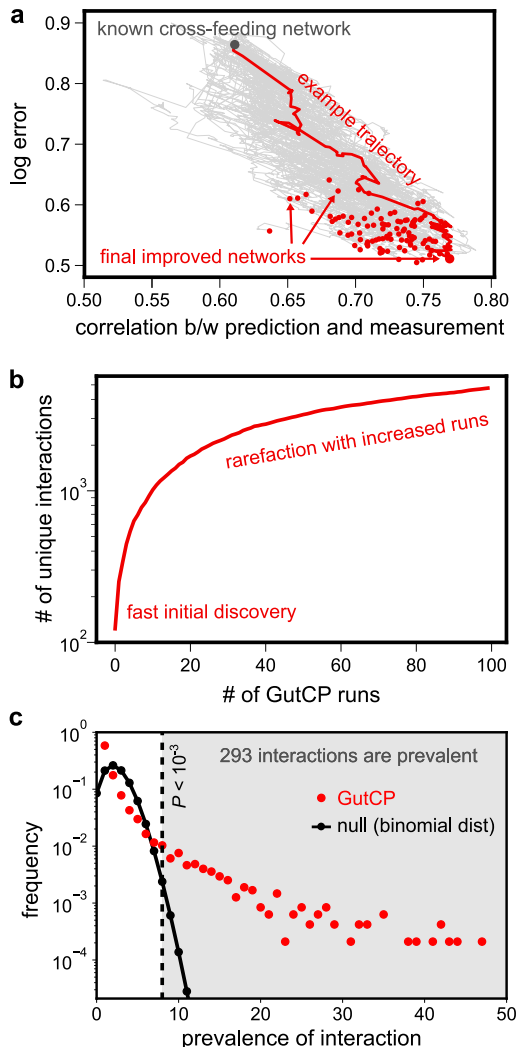


FIG. 2. **Improvement in predictions using GutCP.** **a**, Improvement in log error ( $\log_{10}(\frac{\text{pred}-\text{meas}}{\text{measurement}})$ ) and correlation between the prediction and measured fecal metabolome during 100 typical runs of the GutCP algorithm. The red point at the top left indicates the performance of the original cross-feeding network of Ref.<sup>9</sup>, and the pink points at the bottom right, that of improved networks predicted using GutCP. A trajectory example, highlighting how performance improves over a GutCP run, is shown in red, and others are shown in grey. **b**, Rarefaction curve showing the number of unique cross-feeding interactions discovered by GutCP over 100 runs of the algorithm. **c**, Prevalence of links, i.e., the number of GutCP runs in which they repeatedly appeared (total 100 runs) and for comparison, a corresponding binomial distribution with the same mean (black dotted line).

we used a sample dataset of the gut microbiome and metabolome sampled from 41 human individuals, comprising 221 metabolites and 72 microbial species. We split our sample dataset of 41 individuals into 4 groups, each with 10 individuals (with one exception having 11 individuals). We then ran GutCP to predict cross-feeding interactions four times, each time by using 3 groups to

train the method and find new links (forming the training set), and 1 group to test the model’s performance using the newly predicted links (forming the test set). Finally, we averaged the model’s performance on both the training and test sets to get an estimate of the model’s training and test performance, respectively. This is a standard procedure in machine learning to minimize over-fitting.

We found that both the training and test set performances after using the links predicted by GutCP were significantly better than the baseline given by the original cross-feeding network (Table 1). Specifically, both measures of model performance, namely the logarithmic error and the average correlation, improved by 64% and 20%, respectively, after adding GutCP’s predicted interactions. Additionally, the test set performance was comparable to the training set performance (6% difference; Table 1). This suggests that the cross-feeding interactions inferred by GutCP are not likely to be a result of over-fitting.

**Building a consensus-based atlas of predicted cross-feeding interactions.** Having confirmed that GutCP is unlikely to over-fit data, we pooled the entire sample dataset of 41 individuals and ran 100 independent instances of our prediction algorithm on it; we verified that incorporating more instances did not qualitatively affect our results (Fig. 2b shows a rarefaction curve, which highlights the number of new links discovered by GutCP as we perform more runs the algorithm). Each run of the algorithm resulted in an average of 140 newly predicted cross-feeding interactions. Then, based on consensus from many runs, we assigned a confidence level to each predicted interaction, namely what fraction of GutCP runs it was discovered in. By calculating a null distribution (Fig. 3c, black), which predicts the fraction of GutCP runs where a random link would be discovered by chance, we assigned a  $P$  value to each link, and set a threshold at  $P = 10^{-3}$  (Fig. 3c, red; see Methods for details). Doing so finally resulted in a complete consensus-based atlas of 293 predicted cross-feeding interactions, which we have provided as a resource for experimental verification in supplementary table 1. Fig. 3a shows a condensed version of these interactions obtained from the simulation with the best performance (the trajectory example in Fig. 2a with the lowest log error and highest correlation coefficient) in the form of a matrix; specifically, newly added interactions are in dark colors, and old interactions in faded colors. Fig. S3 shows a complete version of this matrix. Note that some of the predicted interactions in Fig. 3a are unrealistic, e.g., the production of certain sugars like D-Fructose and D-Sorbitol. Such interactions are unlikely to be predicted in repeated simulations, and thus will not be part of the final consensus set. This illustrates the power of pooling results from several simulations to arrive at a set of highly probable predictions.

A network visualization of the complete consensus-based atlas of 293 predicted cross-feeding interactions is

shown in Fig. 3b. Fig. 3b also shows that the network of new interactions have 2 clear type of bacteria: on the left are “producers” and on the right are “consumers”. *Bacteroides*, *Ruminococcus* and *Bifidobacteria* are known byproduct producers in the gut microbiome, and as expected, GutCP predicted more production links for species in these genera<sup>14,37–39</sup>. Consumers, on the other hand (right of Fig. 3b), typically occupy the lower trophic levels, and our model originally under-predicted their abundances. Reasonably, GutCP added several new consumption links to them, allowing these species increased growth and accurately-predicted abundances. Finally, some metabolites, like amino acids (e.g., L-Alanine, L-Tyrosine, and L-Asparagine), short chain fatty acids (e.g., propanoate, valerate, and butyrate) were predicted by GutCP to be mostly produced, not consumed, consistent with the literature<sup>39,40</sup>.

**Large-scale effects and patterns observed in the human gut microbiome.** Equipped with our set of predicted cross-feeding interactions, we examined the extent to which they affected and improved our model’s predictions of the microbe and metabolite levels in the human gut microbiome. We found this improvement indeed significant. For a representative example, see Fig. 4a–d. Here, each panel compares the levels of microbes (Fig. 4a–b) or metabolites (Fig. 4c–d) predicted by the model ( $x$ -axis) with the experimentally measured levels ( $y$ -axis); the closer a point is to the marked line (indicating an exactly correct prediction), the better our predictive power. Even by visual inspection, one can see that the newly predicted interactions bring the points much closer to the line of correct predictions.

By adding new cross-feeding interactions, GutCP not only improves our ability to predict the metabolome, but also nearly doubles the number of metabolites whose levels we could predict (roughly 30 metabolites, in contrast with 17 with the original interactions; see Table 1). GutCP allows microbes to produce new metabolites that were missing from the original set of cross-feeding interactions. These new metabolites were indeed part of the experimentally measured metabolomes for these samples, and we found that we could predict their levels with comparable accuracy (compare Fig. 4d with Fig. 4c). Similarly, GutCP increased the number of microbial species whose levels we could predict. This was especially true of those microbial species, which could not grow given the original interactions (left-most points in Fig. 4a). By inferring the appropriate consumption links for these species, GutCP could also predict their levels correctly (in Fig. 4b, the left-most points moved close to the line of exact predictions).

Because our model mechanistically connects the abundances of microbes and metabolites, we next sought to understand how GutCP enabled such an improvement in the model’s performance. We did this by comparing the change in the prediction error (or systematic bias) of each metabolite (Fig. 4e, white background; blue boxes indi-

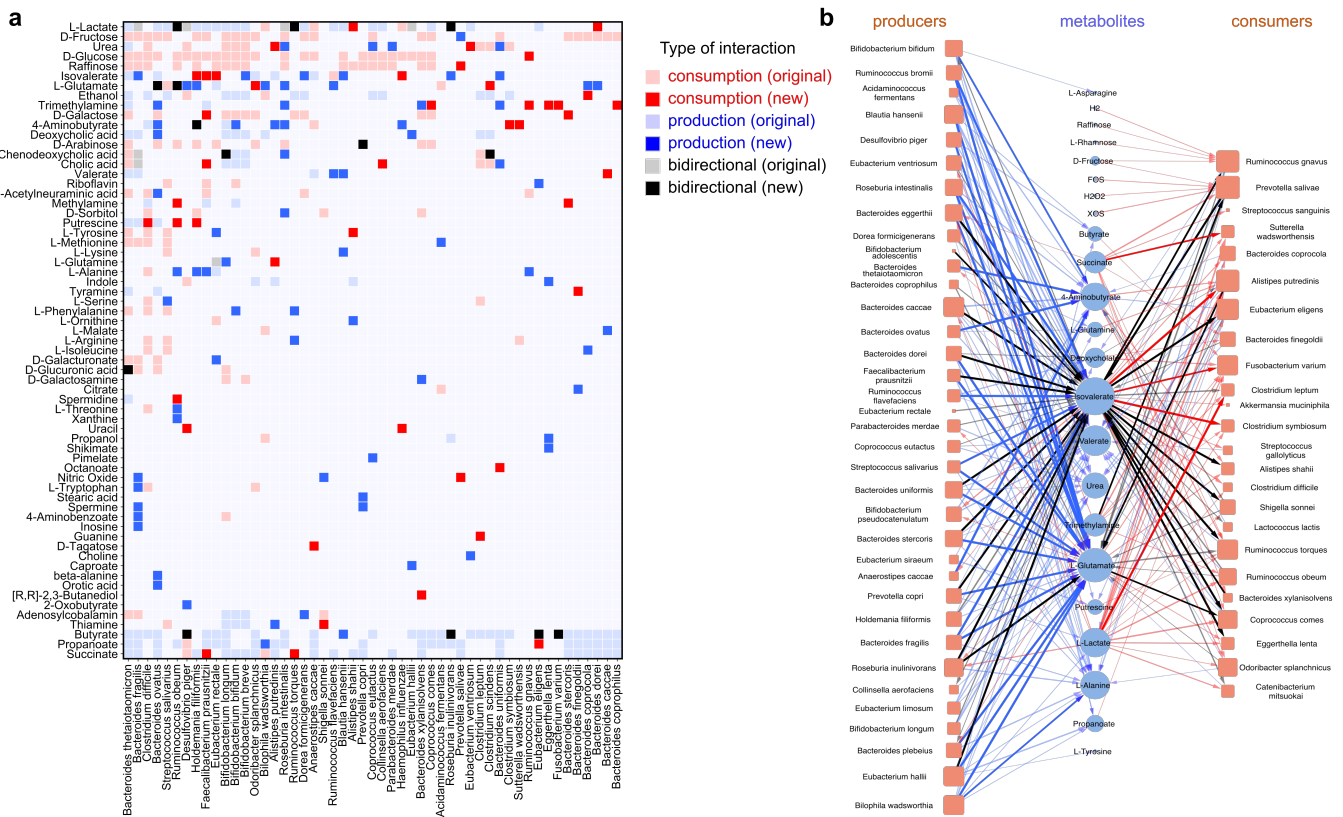


**FIG. 3. New cross-feeding interactions predicted by GutCP.** **a**, Concise matrix representation of the improved cross-feeding network of the gut microbiome predicted by GutCP (the trajectory example in Fig. 2a with the best performance). The rows are metabolites, and columns, microbial species. Faded cells represent the original, known set of cross-feeding interactions, both production (light blue), consumption (light red) and bidirectional links (grey). The new cross-feeding interactions predicted by GutCP are shown in dark colors: production links in dark blue, consumption links in dark red, and bidirectional links in black. **b**, Network of 293 new links predicted by GutCP ( $P$  value  $< 10^{-3}$ ) during 100 independent simulations. Blue nodes represent metabolites, orange are bacteria as in Fig. 1. The size of each node represents its degree. The color of the links is the same as in (a), while the color intensity and link thickness are proportional to the link's confidence, or  $P$  value. For bidirectional links, we represent the direction as that of the link with the smaller  $P$  value.

cate the original predictive error, and red boxes indicate the predictive error after adding GutCP's predictions) with the links that were added for each metabolite (Fig. 3).

We found that the newly predicted interactions had both direct and indirect effects on metabolite levels, and these were crucial for accurate prediction. By direct effects, we mean the following: if a systematically over-predicted (or under-predicted) metabolite was fixed by GutCP by inferring that a new microbe could consume (or produce) it, this new consumption (or production) link had a direct role in that metabolite's accurate prediction. For instance, we noticed that originally, spermidine was over-predicted (Fig. 4e, spermidine in blue); GutCP inferred a new consumption interaction (by *Ruminococcus obeum*; Fig. 3), and this corrected the spermidine level in the metabolome (Fig. 4e, spermidine in red), leading to a direct accurate prediction. Similarly, the amino acid lysine was under-predicted, which was fixed due to GutCP inferring a new production link (by

*Blautia hansenii*; Fig. 3). Sometimes, a metabolite's under- or over-prediction was fixed as a result of GutCP inferring multiple consumption or production links by several different microbial species in tandem (such as for putrescine, for which GutCP inferred 3 consumption links; Fig. 3). With only a subset of the inferred links, the levels of such metabolites still remained under- or over-predicted. Strikingly, we also observed several indirect effects of GutCP's predictions. By indirect effects, we mean that some under- or over-predicted metabolite levels were corrected, even though GutCP inferred no new link to consume or produce it. Instead, the levels were corrected due to the cascading nature of cross-feeding, where the production or consumption of other metabolites by the microbiome could affect the growth of microbes consuming or producing a particular metabolite, thereby indirectly affecting its levels. For example, GutCP inferred no new consumption or production links for 5-Aminovalerate (Fig. 3), but adding other links (such as the consumption of putrescine by *Clostridium*

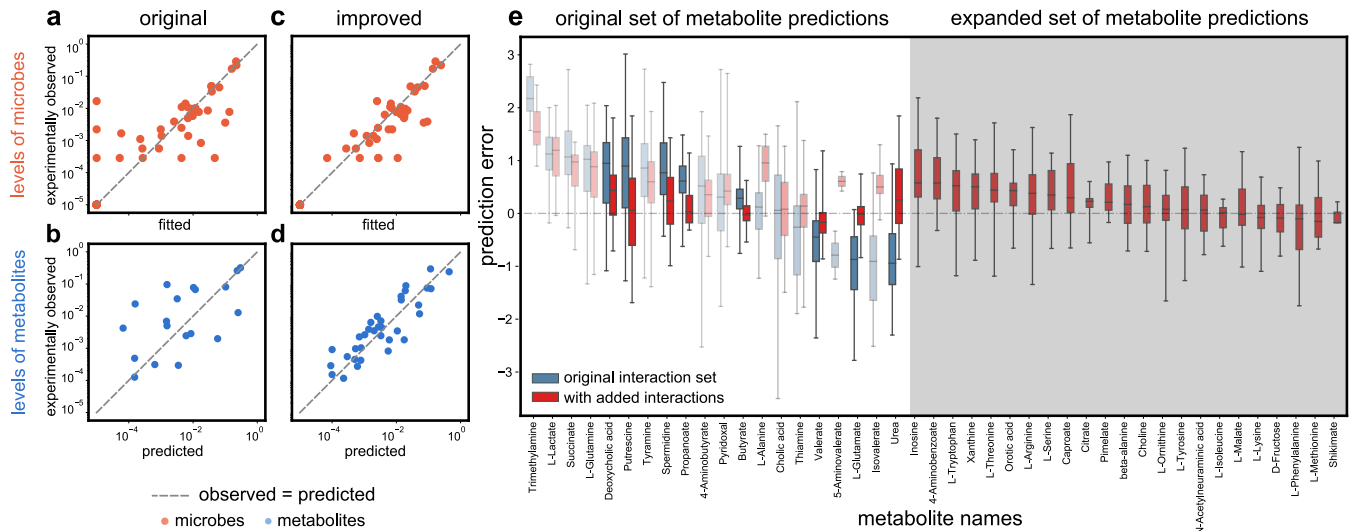


FIG. 4. **The effects of GutCP’s predicted interactions on the gut microbiome and metabolome.** (a–d) Each panel compares the levels of microbial species (a and c; blue) or metabolites (b and d; orange) predicted by our ecological consumer-resource model ( $x$ -axis) with the experimentally measured levels ( $y$ -axis); the closer a point is to the marked line (indicating an exactly correct prediction), the better our predictive power. The predictions using the original, known set of cross-feeding interactions are on the left, and using the additional cross-feeding interactions predicted by GutCP are on the right. **e**, Box plot showing the improvement in prediction error of each metabolite in the fecal metabolome. Prediction errors using the original cross-feeding network are in blue, and those with added interactions predicted by GutCP are in red. Central bars indicate median, boxes and whiskers indicate quartiles, and diamonds indicate outliers beyond the 1.5 inter-quartile range. Metabolites for which GutCP improved predictions highly are shown in solid bold colors for illustration; those with faded colors represent modest improvements. The shaded grey part of the plot shows new metabolites whose levels GutCP helped predict, but the original cross-feeding network could not.

*difficile*) that simultaneously boosts the growth of microbes that produce it, helped solve its original under-prediction. Note that interactions such as these can only be inferred by causal and mechanistic models; this is because they alone can find such emergent, indirect effects of the microbiome on the metabolome.

**Validating the predicted interactions using evidence from genome sequences.** The full set of the interactions we predicted here (293) is quite large, which is why we provide them as a resource to guide experimental efforts in building a more complete list of cross-feeding interactions. While the experimental verification of our predictions is outside the scope of this study, we provide evidence suggesting that our predicted interactions are indeed consistent with the evidence from genome-scale metabolic networks<sup>28,29,41</sup>, which annotates metabolic capabilities directly from genome sequences, but vastly overestimates the number of cross-feeding interactions. To validate the interactions predicted by our algorithm, we calculated the fraction of predicted interactions that were also predicted by sequence based methods (see Methods for details). As a control, we asked: if our predicted interactions were essentially random, what fraction of GutCP’s predictions would still be present in the genome-based predictions? We found that 65% of our predicted interactions were also predicted by genome-

based predictions, much higher than expected by chance (controls had  $\sim 20\%$ ; binomial test,  $P$  value  $2 \times 10^{-8}$ ). This strongly suggests that GutCP’s predicted interactions not only have ecological and biological relevance, but are also consistent with genome annotation results.

## DISCUSSION

Inferring ecological interactions is crucial to building a mechanistic understanding of microbial communities microbiomes<sup>42</sup>. To date, studies that have attempted this have focused on inferring species-species interactions<sup>43–45</sup>. Although knowledge of species-species interactions can be used to predict the possibility of coexistence between microbial species, the interactions themselves are dynamic and depend on environmental conditions<sup>46,47</sup>. This makes them difficult not only to verify, but also to make subsequent predictions with. Here, we have taken an alternative, but more powerful and mechanistic approach: that of inferring species-metabolite interactions (or cross-feeding interactions), which (1) subsume inter-species interactions, (2) no longer depend on environmental conditions, and (3) are simpler to experimentally verify. The new cross-feeding interactions predicted in this paper are a direct reflection of the metabolic capabilities of different microbial species

and are thus easier to test through experiments. Our approach is grounded in a mechanistic model of the gut microbiome<sup>20</sup>, which allows reliable causal inference between the metagenome and metabolome, compared with alternatives that depend merely on correlations between microbes and metabolites<sup>11,48–50</sup>.

Using our algorithm, GutCP, we have provided here an atlas of 293 high-consensus cross-feeding interactions between 72 prominent gut microbial species and 221 gut metabolites. Given the general and broad applicability of GutCP, we anticipate that the access to a larger number of experimental measurements of the gut metagenome and metabolome will help complete the inference of all relevant ecological metabolite-driven interactions in the microbiome. This is because GutCP helps to narrow down and pinpoint those interactions that are most likely to be present, and this is crucial because the number of possible cross-feeding interactions in the gut is extremely large ( $\sim 30,000$ )<sup>29,41</sup>; sampling all possible interactions requires extremely high-throughput experimental tests, far beyond the scope of what is currently possible. Further, genome-based metabolic network reconstruction methods are noisy, and tend to predict more than 10,000 total interactions<sup>29,41</sup>, tens of times more than the ecologically relevant number of interactions in the gut<sup>9</sup>. With the proof-of-concept dataset that we used here, GutCP was able to narrow down this list from 30,000 to about 300, resulting in a 100-fold reduction of the required experimental throughput. We found that 65% of our predicted interactions were supported by the available genomic evidence. While this is still a large number of experimental tests to perform, the complete table of predictions should serve as a resource guiding future experimentally tractable ecological inference in the gut microbiome.

Even though at first glance, GutCP appears similar to gap-filling during flux-balance analysis (FBA)<sup>28,29,41</sup>, there are fundamental differences between these two methods, and both solve very different problems using very different datasets. Gap-filling infers intra-cellular metabolic reactions required for growth of a single microbial species in a particular medium; for this, it uses microbial growth data in specific media. In contrast, our algorithm infers extra-cellular, cross-feeding interactions required to better predict the levels of several microbial species and metabolites simultaneously; for this, it uses a small set of simultaneous measurements of gut metagenomes and metabolomes. One can think of our method as a community-level gap-filling: where each microbial species is effectively a net chemical reaction, and new cross-feeding interactions add new links between species.

GutCP also stands in contrast with previous correlation-based studies to infer microbe-microbe<sup>51–55</sup> and microbe-metabolite associations<sup>11,48–50</sup>. While these approaches are model-free and easy to compute, they lack any mechanistic understanding of the microbiome, and can thus cannot distinguish between direct and indirect

effects of metabolites on microbes. Because of its explicit mechanistic and ecology-guided approach, GutCP can more naturally tell which microbe-metabolite interactions indicate a direct versus an indirect association (see the examples in the Results section). Collectively, this work advances the field of integrative multi-omics, by suggesting a new way to integrate two -omics measurements (metagenomics and metabolomics) through causation, not merely correlation.

## METHODS

**Datasets.** Throughout this study, we used a previously published dataset of simultaneous gut metagenome and fecal metabolome measurements from 41 human individuals<sup>56</sup>; this dataset was used as a proof-of-concept, and was identical to the dataset used to calibrate the ecological consumer-resource model of the gut microbiome in this study (see Wang et al<sup>20</sup> for the complete description of the model and how we processed the dataset). Briefly, the dataset measured 16S rRNA OTU abundances for gut metagenome measurements, and CE-TOF mass spectrometry for quantitative fecal metabolome profile measurements. For the original, known set of cross-feeding interactions, we used a previously published database of experimentally verified and manually curated cross-feeding interactions, created specially for human gut microbiome studies<sup>9</sup>. We mapped the species in this database to the species in our experimental dataset as described previously in Wang et al<sup>20</sup>. To compare our predicted interactions with genome-scale metabolic networks, we obtained semi-automatically reconstructed genome-scale metabolic models from Garza et al<sup>29</sup>; this dataset had over 1,500 genome-scale metabolic models, but we only used those models that mapped to the 72 species and 221 metabolites in our dataset.

**GutCP algorithm.** GutCP uses both a previously published ecological consumer-resource model and machine learning optimization techniques. The ecological model we used in this manuscript was a previously published model that we developed, namely a trophic model of the human gut microbiome<sup>20</sup>. Our trophic model follows the discrete and stepwise flow of metabolite consumption and subsequent byproduct generation by microbial species in the gut. By knowing which species consume and produce which metabolites, this model can predict the fecal metabolome with relatively high accuracy. Originally, we used the set of consumption and production abilities of each microbial species from a manually curated database, as described above. GutCP assumes that we can discover, infer and predict new cross-feeding interactions in the gut that are not present in the manually-curated database by identifying that set of new interactions that further improve our estimate of the fecal metabolome. GutCP proceeds in discrete time steps, where each step resembles a Markov Chain Monte Carlo (MCMC) optimization method<sup>33</sup>, but with a few key differences. GutCP consists of five major steps, detailed as follows.

*Step 1: Setup, and measuring systematic biases.* We start with an initial cross-feeding network, derived from the manually-curated database of interactions in the gut microbiome. We use our consumer-resource model with this original network on our dataset, and generate a set of metabolome estimates. We then calculate a systematic bias,  $b_i$ , for each metabolite and microbe predicted by the model, namely the difference between the predicted and experimentally measured levels, averaged over all samples in the dataset, as follows:

$$b_i = \frac{1}{N_s} \sum_{\alpha=1}^{N_s} (\log_{10}(p_{\alpha,i}) - \log_{10}(m_{\alpha,i})), \quad (1)$$

where  $p_{\alpha,i}$  and  $m_{\alpha,i}$  represent the predicted levels and experimentally measured levels, respectively, for sample  $\alpha$  and microbe or

metabolite,  $i$ .  $N_s = 41$  is the number of samples in the dataset. We measure bias in logarithmic units to estimate the average order of magnitude of the bias. A large, positive bias indicates a systematic over-prediction, and a large, negative bias, a systematic under-prediction.

*Step 2: Calculating priors and proposing a new link.* GutCP then uses the initial systematic bias measurements to calculate a likelihood of missing links for a particular metabolite or microbial species. It assigns this likelihood by considering the magnitude and sign of the systematic bias for each microbe and metabolite. Specifically, it assigns the probability  $\mathcal{P}_{i,j}^{\text{con}}$ , that species  $i$  consumes metabolite  $j$ , if species  $i$  is under-predicted and/or if metabolite  $j$  is over-predicted, as follows:

$$\mathcal{P}_{i,j}^{\text{con}} \propto e^{-3 \cdot (b_i - b_j)} + \kappa, \quad (2)$$

where  $b_i$  and  $b_j$  are the systematic biases of species  $si$  and metabolite  $j$  measured using equation (1), and  $\kappa = 0.1$  is an arbitrarily chosen constant to ensure the addition of indirect cross-feeding interactions that do not depend on the levels of  $i$  and  $j$  specifically. Similarly, GutCP assigns the probability  $\mathcal{P}_{i,j}^{\text{pro}}$ , that species  $i$  produces metabolite  $j$ , if metabolite  $j$  is under-predicted, as follows:

$$\mathcal{P}_{i,j}^{\text{pro}} \propto e^{-3 \cdot b_j} + \kappa, \quad (3)$$

where the symbols have the same meaning as in equations (1) and (2). All associated prior probabilities on new links,  $\mathcal{P}^{\text{con}}$  and  $\mathcal{P}^{\text{pro}}$ , are normalized to sum up to 1. GutCP then proposes the addition of a new link to the current cross-feeding network (originally, the given network) by choosing one link randomly using this prior probability distribution.

*Step 3: Evaluating objective function with proposed link.* GutCP re-calculates the systematic bias for each metabolite and microbe predicted by our consumer-resource model, this time using the cross-feeding network with the newly proposed link. It then incorporates it into an objective function,  $E$ , defined as follows:

$$E = \frac{1}{N_s} \frac{1}{\mathcal{M}} \sum_{\alpha=1}^{N_s} \sum_{i=1}^{\mathcal{M}} |\log_{10}(p_{\alpha,i}) - \log_{10}(m_{\alpha,i})| \quad (4)$$

$$+ \lambda_{\text{reg}} \cdot \mathcal{N}_{\text{added}} - \lambda_{\text{reward}} \cdot \mathcal{M},$$

where  $\mathcal{M}$  is the number of metabolites predicted by the model that overlap with the experimentally measured metabolomes, and  $\mathcal{N}_{\text{added}}$  is the total number of links added by GutCP.  $\lambda_{\text{reg}}$  is a hyper-parameter that penalizes the addition of new links by a fixed amount, and  $\lambda_{\text{reward}}$  is a hyper-parameter that encourages the algorithm to predict new metabolite levels that overlap with the experimentally measured metabolites. Specifically, we calculate  $E$  both before and after the addition of the newly proposed link, and measure the difference between them,  $\Delta E$ .

*Step 4: Accepting or rejecting the newly proposed link.* GutCP accepts the newly proposed link with a probability proportional to the reduction in the value of the objective function,  $\Delta E$ . Essentially, GutCP accepts the link if  $E$  reduces with a high probability, and accepts it if it increases with only a small probability; this is a common choice in such optimization algorithms, and in this case helps GutCP find links that combine with others later to together improve predictions as a pair. The probability of accepting a newly proposed link is  $\mathcal{P}^{\text{accept}} \propto e^{(-\frac{\Delta E}{kT})}$  where  $\frac{1}{kT} = 5000$  is a calibrated effective energy, representing the effect of a randomly chosen link on the objective function.

*Step 5: Stopping criteria.* We then repeat steps 2 to 4 multiple times iteratively. GutCP stops when the change in the objective function  $E$  due to carefully chosen links starts becoming comparable to changes due to a randomly added link. It does this by comparing the overall change in  $E$  over the past 500 iterations. If

this change is comparable to the change over 500 randomly chosen steps, GutCP stops.

**Calibration of hyper-parameters.** To optimize the performance of GutCP's link discovery procedure, we calibrated the two hyper-parameters in the objective function in equation (4), namely  $\lambda_{\text{reg}}$  and  $\lambda_{\text{reward}}$ . For this, we chose a large range of these hyper-parameters, between  $10^{-4}$  and  $10^{-2}$  for  $\lambda_{\text{reg}}$ , and  $10^{-4}$  and  $10^{-1}$  for  $\lambda_{\text{reward}}$ , each in multiples of 10. For each pair of hyper-parameter values in this range, we ran GutCP and assessed its average performance at the end of 100 runs, where we used the same three measures of performance as throughout the text: (1) the correlation between the predicted and experimentally measured metabolome, (2) the log error (see main text), and (3) the number of metabolites in the measured metabolome predicted by our ecological consumer-resource model (Fig. S4 and S5). We chose those values of the hyper-parameters that simultaneously achieved the best combination of performances on all three measures. We finally chose the values  $\lambda_{\text{reg}} = 10^{-3}$  and  $\lambda_{\text{reward}} = 10^{-3}$  and used them for the results shown in the rest of this manuscript.

**Obtaining the consensus-based atlas of predicted cross-feeding interactions.** To calculate a consensus-based set of cross-feeding predictions, we performed 100 independent runs of GutCP. For every link predicted over all the 100 runs, we measured its prevalence, that is, the fraction of runs in which GutCP discovered the link. To determine which links were inferred by GutCP more often than expected purely by chance, we also calculated a null distribution, which was equivalent to a binomial distribution; in the null, the probability of a link being discovered by chance was the average number of links discovered in any individual run ( $\sim 140$ ), divided by the total number of discoverable links. We used the null distribution to assign a  $P$  value to each discovered link, and assigned those links with  $P < 10^{-3}$  as part of our consensus based set of cross-feeding predictions (supplementary table 1). Increasing or decreasing the  $P$  value threshold within the order of magnitude did not change the number of consensus predictions by more than 5%.

**Validating the predicted interactions using genome-scale metabolic models.** To validate the set of interactions predicted by GutCP, we used genome-scale metabolic models, which make predictions about metabolic reactions from genome sequences, but are known to overestimate the number of metabolic reactions between species and metabolites in the environment. We used the dataset from Garza et al<sup>29</sup>, which contained over 1,500 genome-scale metabolic models (GSMMs). We extracted only those models which were relevant to the 72 microbial species in our dataset. From each GSMM, we specifically extracted those reactions that were marked as extracellular, since those represented the consumption and production links that we are interested in. During extraction, we chose only those reactions which involved metabolites for which we had experimental measurements in our dataset. Doing this gave us a full list of all genome-based cross-feeding interactions relevant to the species and metabolites of interest. We then measured the fraction of cross-feeding interactions predicted by GutCP that were presented in this list of GSMM-based predictions.

**Statistics.** To calculate correlation coefficients throughout the study, we used Pearson's correlation coefficient. Wherever we used  $P$  values, we explained in the Methods how we calculated them, since for all such measurements in the study, we calculated the associated null distributions from scratch. All statistical tests were performed using standard numerical and scientific computing libraries in the Python programming language (version 3.5.2).

**Code availability.** The code for both our simulations and statistical analysis, and for the GutCP algorithm, can be downloaded from: [https://github.com/maslov-group/ML\\_human\\_gut](https://github.com/maslov-group/ML_human_gut).

- <sup>1</sup> I. Cho and M. J. Blaser, *Nature Reviews Genetics* **13**, 260 (2012).
- <sup>2</sup> M. J. Blaser and S. Falkow, *Nature Reviews Microbiology* **7**, 887 (2009).
- <sup>3</sup> H. M. P. Consortium *et al.*, *Nature* **486**, 207 (2012).
- <sup>4</sup> J. Qin, R. Li, J. Raes, M. Arumugam, K. S. Burgdorf, C. Manichanh, T. Nielsen, N. Pons, F. Levenez, T. Yamada, *et al.*, *nature* **464**, 59 (2010).
- <sup>5</sup> J. Qin, Y. Li, Z. Cai, S. Li, J. Zhu, F. Zhang, S. Liang, W. Zhang, Y. Guan, D. Shen, *et al.*, *Nature* **490**, 55 (2012).
- <sup>6</sup> C. A. Lozupone, J. I. Stombaugh, J. I. Gordon, J. K. Jansson, and R. Knight, *Nature* **489**, 220 (2012).
- <sup>7</sup> J. A. Gilbert, R. A. Quinn, J. Debelius, Z. Z. Xu, J. Morton, N. Garg, J. K. Jansson, P. C. Dorrestein, and R. Knight, *Nature* **535**, 94 (2016).
- <sup>8</sup> J. C. Clemente, L. K. Ursell, L. W. Parfrey, and R. Knight, *Cell* **148**, 1258 (2012).
- <sup>9</sup> J. Sung, S. Kim, J. J. T. Cabatbat, S. Jang, Y.-S. Jin, G. Y. Jung, N. Chia, and P.-J. Kim, *Nature communications* **8**, 15393 (2017).
- <sup>10</sup> A. Van Wey, A. Cookson, N. Roy, W. McNabb, T. Soboleva, and P. Shorten, *International journal of food microbiology* **191**, 172 (2014).
- <sup>11</sup> E. A. Franzosa, A. Sirota-Madi, J. Avila-Pacheco, N. Fornelos, H. J. Haiser, S. Reinker, T. Vatanen, A. B. Hall, H. Mallick, L. J. McIver, *et al.*, *Nature microbiology* **4**, 293 (2019).
- <sup>12</sup> W. Scheppach, *Gut* **35**, S35 (1994).
- <sup>13</sup> W. Roediger, *Gut* **21**, 793 (1980).
- <sup>14</sup> P. Vernocchi, F. Del Chierico, and L. Putignani, *Frontiers in microbiology* **7**, 1144 (2016).
- <sup>15</sup> S. H. Duncan, A. Belenguer, G. Holtrop, A. M. Johnstone, H. J. Flint, and G. E. Lobley, *Appl. Environ. Microbiol.* **73**, 1073 (2007).
- <sup>16</sup> A. Shafquat, R. Joice, S. L. Simmons, and C. Huttenhower, *Trends in microbiology* **22**, 261 (2014).
- <sup>17</sup> R. Muñoz-Tamayo, B. Laroche, E. Walter, J. Doré, and M. Leclerc, *Journal of theoretical biology* **266**, 189 (2010).
- <sup>18</sup> H. Kettle, P. Louis, G. Holtrop, S. H. Duncan, and H. J. Flint, *Environmental microbiology* **17**, 1615 (2015).
- <sup>19</sup> R. Marsland III, W. Cui, J. Goldford, A. Sanchez, K. Korolev, and P. Mehta, *PLoS computational biology* **15**, e1006793 (2019).
- <sup>20</sup> T. Wang, A. Goyal, V. Dubinkina, and S. Maslov, *PLOS Computational Biology* **15**, 1 (2019).
- <sup>21</sup> M. A. Fischbach and J. L. Sonnenburg, *Cell host & microbe* **10**, 336 (2011).
- <sup>22</sup> A. Goyal, *PLoS genetics* **14**, e1007763 (2018).
- <sup>23</sup> R. Van der Meulen, L. Makras, K. Verbrugghe, T. Adriany, and L. De Vuyst, *Appl. Environ. Microbiol.* **72**, 1006 (2006).
- <sup>24</sup> G. Falony, A. Vlachou, K. Verbrugghe, and L. De Vuyst, *Appl. Environ. Microbiol.* **72**, 7835 (2006).
- <sup>25</sup> A. Amaretti, T. Bernardi, E. Tamburini, S. Zanoni, M. Lomma, D. Matteuzzi, and M. Rossi, *Appl. Environ. Microbiol.* **73**, 3637 (2007).
- <sup>26</sup> S. Shoaie, F. Karlsson, A. Mardinoglu, I. Nookaew, S. Bordel, and J. Nielsen, *Scientific reports* **3**, 2532 (2013).
- <sup>27</sup> A. Heinken, S. Sahoo, R. M. Fleming, and I. Thiele, *Gut microbes* **4**, 28 (2013).
- <sup>28</sup> S. Magnúsdóttir, A. Heinken, L. Kutt, D. A. Ravcheev, E. Bauer, A. Noronha, K. Greenhalgh, C. Jäger, J. Baginska, P. Wilmes, *et al.*, *Nature biotechnology* **35**, 81 (2017).
- <sup>29</sup> D. R. Garza, M. C. van Verk, M. A. Huynen, and B. E. Dutilh, *Nature microbiology* **3**, 456 (2018).
- <sup>30</sup> E. J. O'Brien, J. M. Monk, and B. O. Palsson, *Cell* **161**, 971 (2015).
- <sup>31</sup> M. A. Oberhardt, J. Puchałka, K. E. Fryer, V. A. M. Dos Santos, and J. A. Papin, *Journal of bacteriology* **190**, 2790 (2008).
- <sup>32</sup> A. R. Pacheco, M. Moel, and D. Segre, *Nature communications* **10**, 103 (2019).
- <sup>33</sup> C. Andrieu, N. De Freitas, A. Doucet, and M. I. Jordan, *Machine learning* **50**, 5 (2003).
- <sup>34</sup> K. P. Murphy, *Machine learning: a probabilistic perspective* (MIT press, 2012).
- <sup>35</sup> O. S. Venturelli, A. V. Carr, G. Fisher, R. H. Hsu, R. Lau, B. P. Bowen, S. Hromada, T. Northen, and A. P. Arkin, *Molecular systems biology* **14** (2018).
- <sup>36</sup> A. Goyal and S. Maslov, *Physical Review Letters* **120**, 158102 (2018).
- <sup>37</sup> A. Rivière, M. Selak, D. Lantin, F. Leroy, and L. De Vuyst, *Frontiers in microbiology* **7**, 979 (2016).
- <sup>38</sup> N. T. Porter and E. C. Martens, *Cell host & microbe* **19**, 745 (2016).
- <sup>39</sup> I. Rowland, G. Gibson, A. Heinken, K. Scott, J. Swann, I. Thiele, and K. Tuohy, *European journal of nutrition* **57**, 1 (2018).
- <sup>40</sup> S. Sanna, N. R. van Zuydam, A. Mahajan, A. Kurilshikov, A. V. Vila, U. Vösa, Z. Mujagic, A. A. Masclee, D. M. Jonkers, M. Oosting, *et al.*, *Nature genetics* **51**, 600 (2019).
- <sup>41</sup> L. Heirendt, S. Arreckx, T. Pfau, S. N. Mendoza, A. Richelle, A. Heinken, H. S. Haraldsdóttir, J. Wachowiak, S. M. Keating, V. Vlasov, *et al.*, *Nature protocols* **14**, 639 (2019).
- <sup>42</sup> M. Kumar, B. Ji, K. Zengler, and J. Nielsen, *Nature microbiology* **4**, 1253 (2019).
- <sup>43</sup> R. R. Stein, V. Bucci, N. C. Toussaint, C. G. Buffie, G. Rättsch, E. G. Pamer, C. Sander, and J. B. Xavier, *PLoS computational biology* **9**, e1003388 (2013).
- <sup>44</sup> Y. Xiao, M. T. Angulo, J. Friedman, M. K. Waldor, S. T. Weiss, and Y.-Y. Liu, *Nature communications* **8**, 2042 (2017).
- <sup>45</sup> D. S. Maynard, Z. R. Miller, and S. Allesina, *bioRxiv*, 598326 (2019).
- <sup>46</sup> B. Momeni, L. Xie, and W. Shou, *Elife* **6**, e25051 (2017).
- <sup>47</sup> S. Vet, S. de Buyl, K. Faust, J. Danckaert, D. Gonze, and L. Gelens, *PloS one* **13** (2018).
- <sup>48</sup> R. Steuer, J. Kurths, O. Fiehn, and W. Weckwerth, *Bioinformatics* **19**, 1019 (2003).
- <sup>49</sup> D. Camacho, A. De La Fuente, and P. Mendes, *Metabolomics* **1**, 53 (2005).
- <sup>50</sup> C. Noecker, H.-C. Chiu, C. P. McNally, and E. Borenstein, *mSystems* **4** (2019), 10.1128/mSystems.00579-19, <https://msystems.asm.org/content/4/6/e00579-19.full.pdf>.
- <sup>51</sup> L. R. Dice, *Ecology* **26**, 297 (1945).
- <sup>52</sup> K. Faust, J. F. Sathirapongsasuti, J. Izard, N. Segata, D. Gevers, J. Raes, and C. Huttenhower, *PLoS computational biology* **8** (2012).
- <sup>53</sup> J. Friedman and E. J. Alm, *PLoS computational biology* **8** (2012).

- <sup>54</sup> N. Connor, A. Barberán, and A. Clauset, PloS one **12** (2017).
- <sup>55</sup> A. Carr, C. Diener, N. S. Baliga, and S. M. Gibbons, The ISME journal **13**, 2647 (2019).
- <sup>56</sup> J. Kisuse, O. La-ongkham, M. Nakphaichit, P. Therdtatha, R. Momoda, M. Tanaka, S. Fukuda, S. Popluechai, K. Kespechara, K. Sonomoto, *et al.*, Frontiers in microbiology **9** (2018).

**Acknowledgements.** We thank Ananthan Nambiar for help with interpreting evidence from genome sequences. A.G. is supported by the Gordon and Betty Moore Foundation as a Physics of Living Systems Fellow through grant number GBMF4513.

**Author contributions.** S.M. designed the research and supervised the study; T.W. and A.G. performed simulations and calculations. V.D. performed data curation. All authors devised the study and wrote the paper.

**Interests statement.** The authors declare no competing interests.

Supplementary Figures  
Ecology-guided prediction of cross-feeding interactions  
in the human gut microbiome

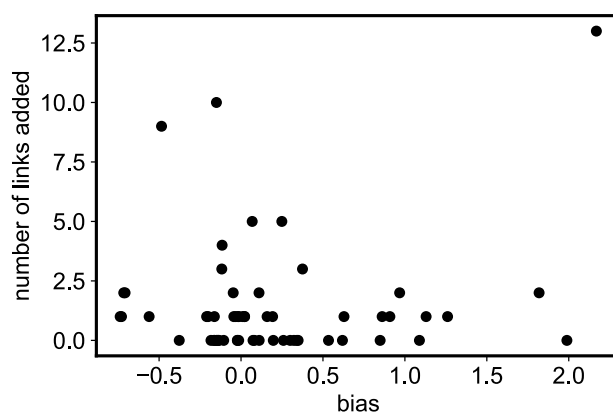


FIG. S1. **No correlation between the prior metabolite systematic bias and the number links added related to the metabolite.** Each point represents a metabolite. Results are shown for one run of GutCP. The Pearson correlation coefficient between the two quantities is 0.15, and the  $P$  value is 0.24, which is not significant.

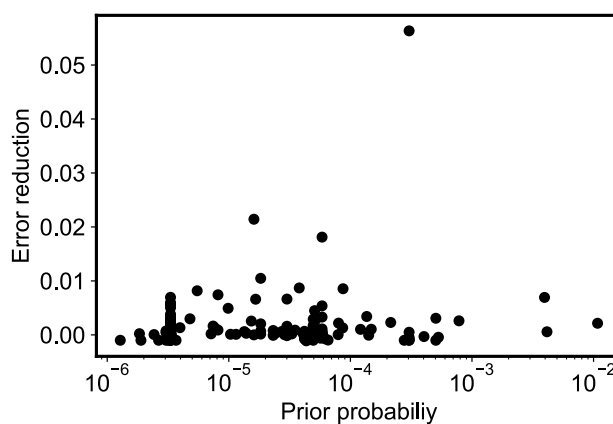


FIG. S2. **No correlation between the prior metabolite probability and the error reduction induced by the added links related to the metabolite.** Each point represents a metabolite. Results are shown for one run of GutCP. The Pearson correlation coefficient between the two quantities is 0.03, and the  $P$  value is 0.74, which is not significant.



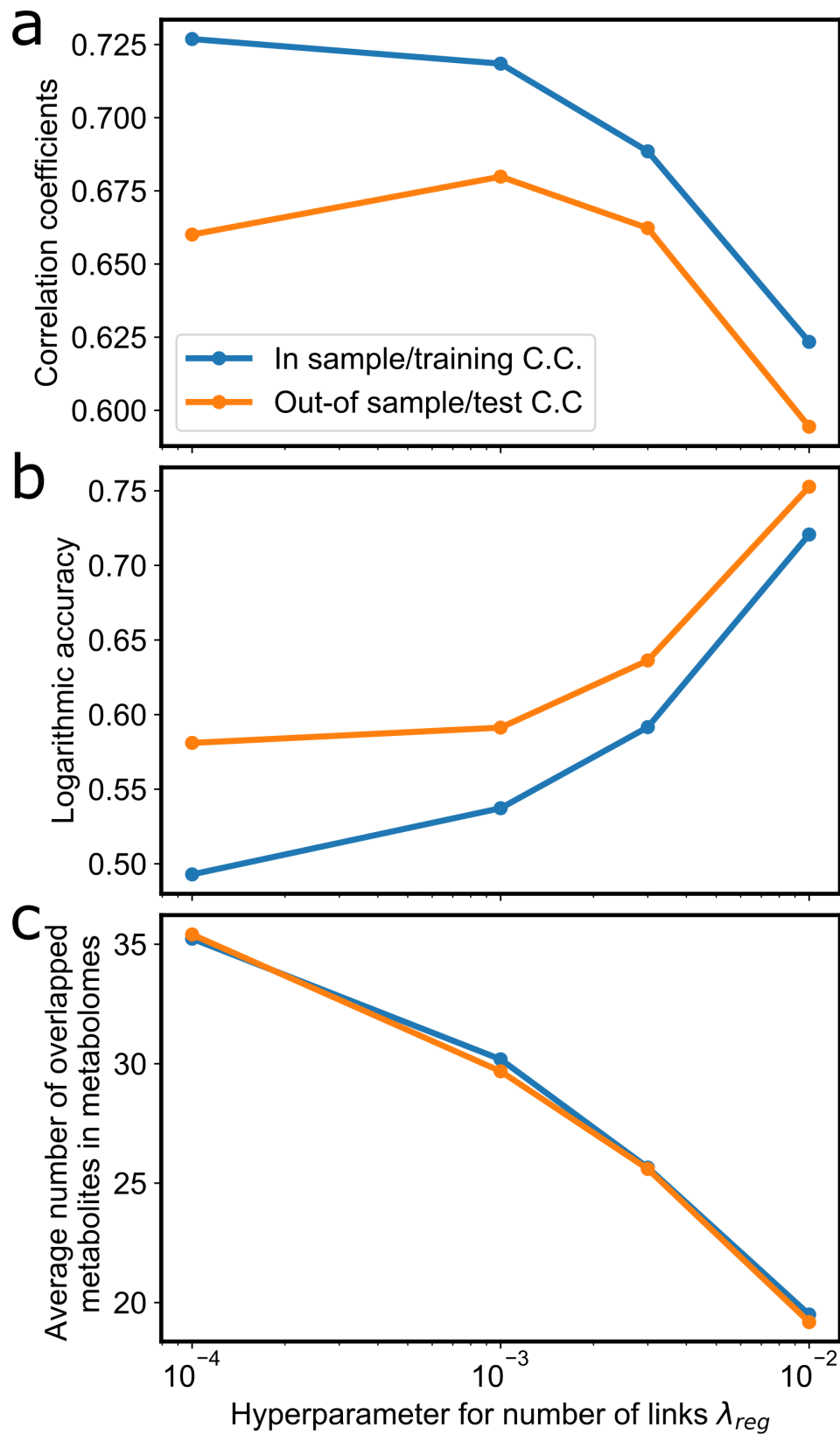


FIG. S4. **The effect of the hyper-parameter for the number of links  $\lambda_{reg}$  on model performance.** Results are shown for one run of GutCP. The other hyper-parameter for rewarding the number of overlapped metabolites  $\lambda_{reward}$  is fixed as  $10^{-3}$  (see Methods).

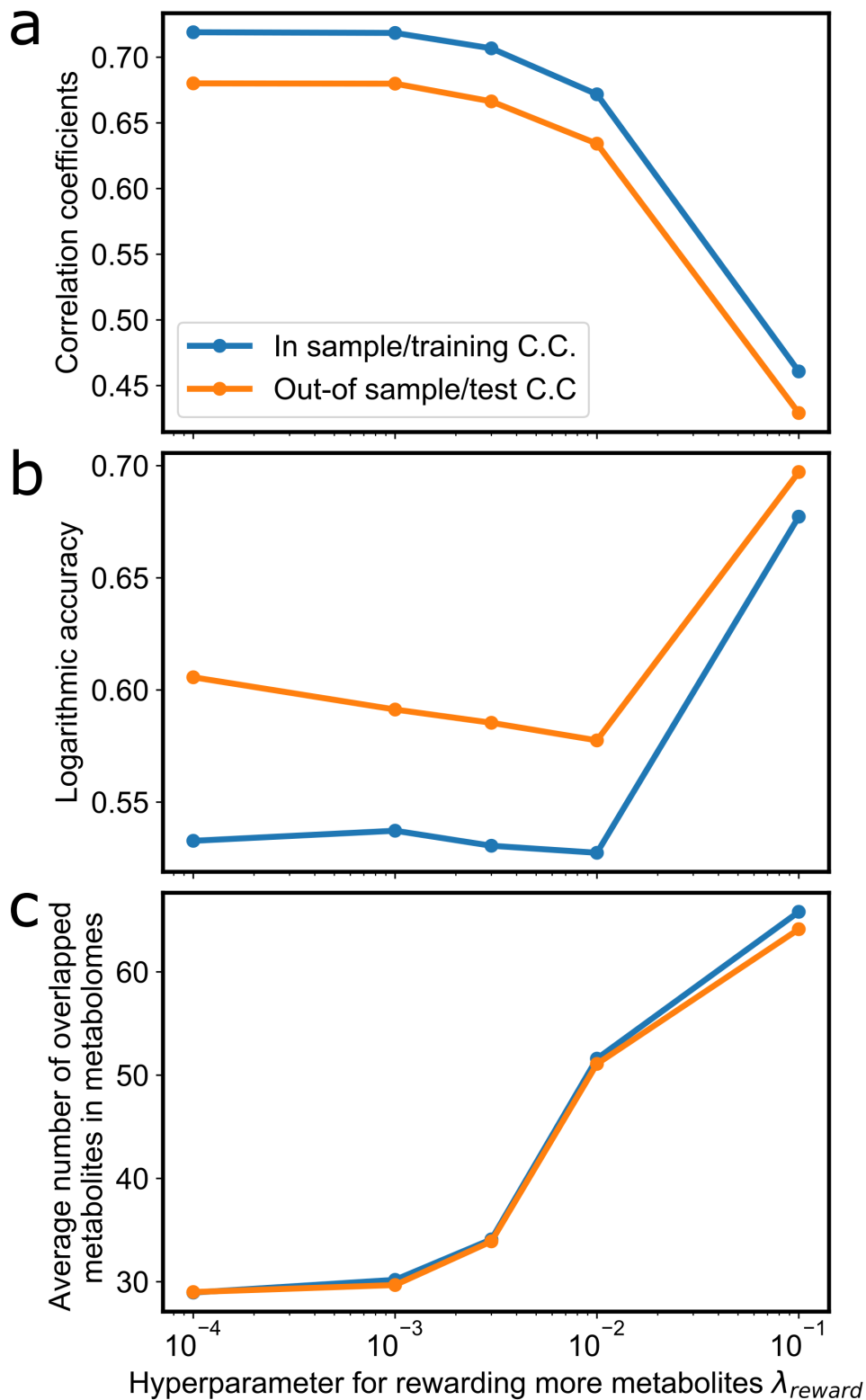
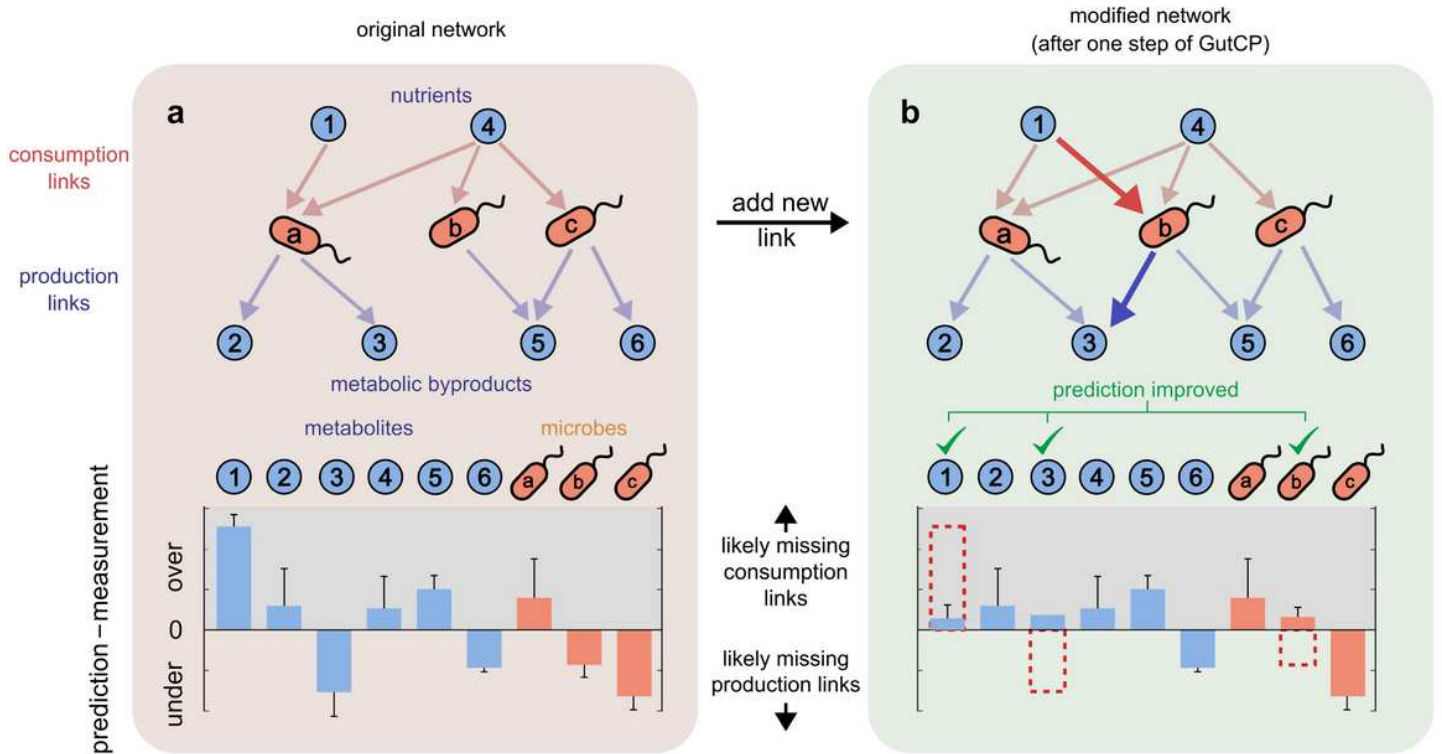


FIG. S5. **The effect of the hyper-parameter for rewarding the number of overlapped metabolites  $\lambda_{reward}$  on model performance.** Results are shown for one run of GutCP. The other hyper-parameter for the number of links  $\lambda_{reg}$  is fixed as  $10^{-3}$  (see Methods).

# Figures



**Figure 1**

Overview of the GutCP algorithm. a, Schematic of the original set of known cross-feeding interactions (top) and bar plot of the prediction error for each metabolite and microbe (bottom). The cross-feeding interactions are represented as a network, whose nodes are either metabolites (cyan circles) or microbial species (orange ellipses), and directed links represent abilities of different species to consume (red arrows) and produce (blue arrows) individual metabolites. b, GutCP adds a new consumption link (red) and production link (blue) as added links reduce the prediction errors for metabolites and microbes.

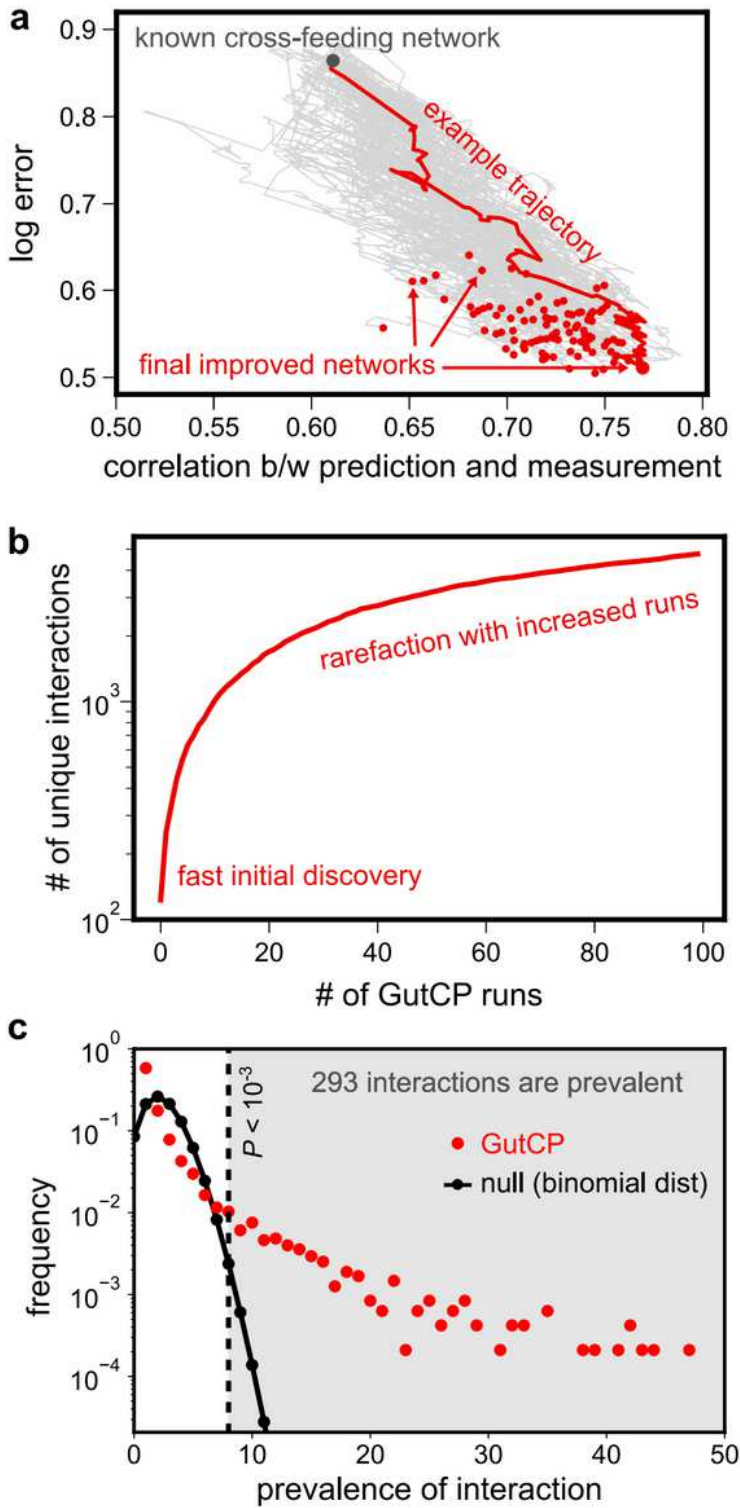


**Figure 2**

Improvement in predictions using GutCP. a, Improvement in log error ( $\log_{10}(\text{pred-meas measurement})$ ) and correlation between the prediction and measured fecal metabolome during 100 typical runs of the GutCP algorithm. The red point at the top left indicates the performance of the original crossfeeding network of Ref.9, and the pink points at the bottom right, that of improved networks predicted using GutCP. A trajectory example, highlighting how performance improves over a GutCP run, is shown in red,

and others are shown in grey. b, Rarefaction curve showing the number of unique cross-feeding interactions discovered by GutCP over 100 runs of the algorithm. c, Prevalence of links, i.e., the number of GutCP runs in which they repeatedly appeared (red dots; total 100 runs) and for comparison, a corresponding binomial distribution with the same mean (black dotted line).

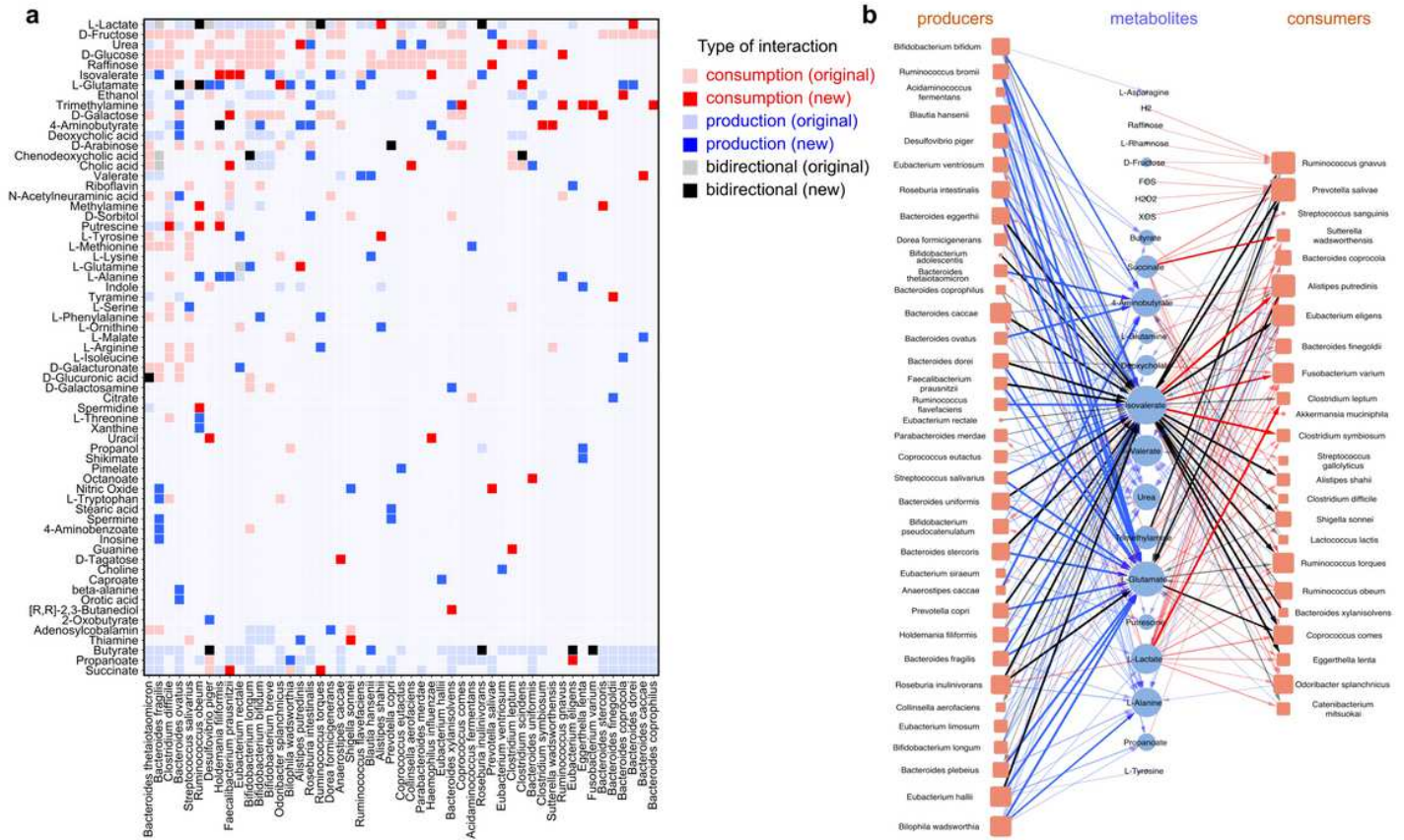


**Figure 3**

New cross-feeding interactions predicted by GutCP. a, Concise matrix representation of the improved crossfeeding network of the gut microbiome predicted by GutCP (the trajectory example in Fig. 2a with the best performance). The rows are metabolites, and columns, microbial species. Faded cells represent the original, known set of cross-feeding interactions, both production (light blue), consumption (light red) and bidirectional links (grey). The new cross-feeding interactions predicted by GutCP are shown in dark colors: production links in dark blue, consumption links in dark red, and bidirectional links in black. b, Network of 293 new links predicted by GutCP ( $P$  value  $< 10^{-3}$ ) during 100 independent simulations. Blue nodes represent metabolites, orange are bacteria as in Fig. 1. The size of each node represents its degree. The color of the links is the same as in (a), while the color intensity and link thickness are proportional to the link's confidence, or  $P$  value. For bidirectional links, we represent the direction as that of the link with the smaller  $P$  value.

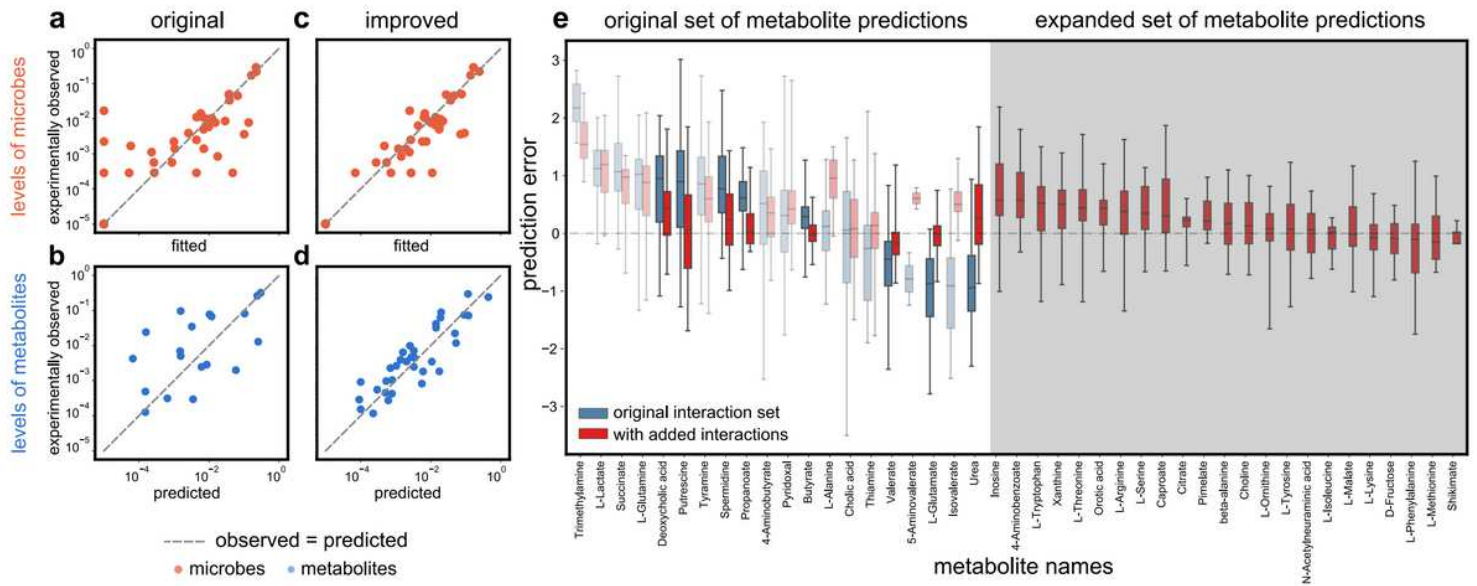


**Figure 4**

The effects of GutCP's predicted interactions on the gut microbiome and metabolome. (a–d) Each panel compares the levels of microbial species (a and c; blue) or metabolites (b and d; orange) predicted by our ecological consumer-resource model (x-axis) with the experimentally measured levels (y-axis); the closer a point is to the marked line (indicating an exactly correct prediction), the better our predictive power. The predictions using the original, known set of cross-feeding interactions are on the left, and using the additional cross-feeding interactions predicted by GutCP are on the right. e, Box plot showing the improvement in prediction error of each metabolite in the fecal metabolome. Prediction errors using the original cross-feeding network are in blue, and those with added interactions predicted by GutCP are in red. Central bars indicate median, boxes and whiskers indicate quartiles, and diamonds indicate outliers beyond the 1.5 inter-quartile range. Metabolites for which GutCP improved predictions highly are shown in solid bold colors for illustration; those with faded colors represent modest improvements. The shaded grey part of the plot shows new metabolites whose levels GutCP helped predict, but the original cross-feeding network could not.

## Supplementary Files

This is a list of supplementary files associated with this preprint. Click to download.

- [S1.png](#)
- [S2.png](#)
- [S3.png](#)
- [S4.png](#)
- [S5.png](#)